CRYSTAL GROWTH & DESIGN

Communication

pubs.acs.org/crystal

Pressure-Induced Crystallization from Amorphous Calcium Carbonate

Toru Yoshino,*[,†] Koji Maruyama,[‡] Hiroyuki Kagi,[‡] Masayuki Nara,[§] and Jeong Chan Kim[∥]

[†]Tokyo Metropolitan Industrial Technology Research Institute, 2-4-10 Aomi, Koto-ku, Tokyo 135-0064, Japan

[‡]Geochemical Research Center (GCRC), Graduate School of Science, The University of Tokyo, 7-3-1 Hongo, Bunkyo-ku, Tokyo 113-0033, Japan

[§]Laboratory of Chemistry, College of Liberal Arts and Sciences, Tokyo Medical and Dental University, 2-8-30 Kounodai, Ichikawa, Chiba 272-0827, Japan

[∥]CO_2 Geological Storage Research Team, Korea Institute of Geoscience and Mineral Resources (KIGAM), 92 Gwahang-no, Yuseong-gu, Daejeon 305-350, Korea

Supporting Information

ABSTRACT: This report describes a newly observed phenomenon: pressure-induced crystallization from amorphous calcium carbonate (ACC). Synthetic ACC samples were pressurized up to 800 MPa at room temperature. Then crystallization of vaterite and calcite was observed from X-ray diffraction patterns. The crystallization pressure depends on the H_2O contents of ACCs. The ACC samples with high-H_2O content (21 wt %), middle-H_2O content (17 wt %), and low-H_2O content (10 wt %) underwent crystallization at pressures higher than 240 MPa, 400 MPa, and 640 MPa, respectively. These results indicate that H_2O in the ACC serves an important role in the crystallization process and that we should treat ACC carefully in preparation for analyses such as infrared spectroscopy to obtain the intrinsic information related to amorphous materials.

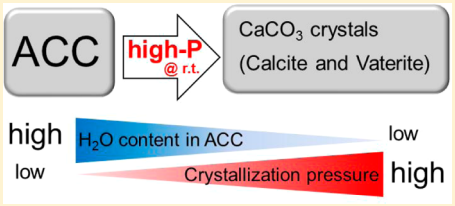

Amorphous calcium carbonate (ACC, $CaCO_3{\cdot}nH_2O$), a metastable hydrous phase of calcium carbonate, is known as a precursor material of crystalline phases of calcium carbonate: calcite, aragonite, and vaterite.[1−4] In nature, ACC can be found as biominerals produced by living organisms.[3,5−12]

In the synthesis of calcium carbonate, ACC appears at an early stage of precipitation from a supersaturated solution of $CaCO_3$.[1,4,13−16] The precipitated ACC crystallizes through the dissolution−precipitation process in an aqueous solution or under humid conditions when it is not stabilized by an additive.[1,4,13] Recently, the crystallization from an aggregated ACC has become known to be inducible by polymers and templates (e.g., polyaspartate and carboxylate-functionalized SAMs).[16−18] In this process, crystallized products maintain the original shape of the aggregated ACC. Therefore, this process is regarded as a solid-state-like transformation. These crystallization processes occur in aqueous solution and require water, which mediates the reactions. However, ACC can be crystallized at high temperature (>570 K)[19] and the thermal crystallization of ACC needs no water.

Herein, we present a new crystallization process from ACC, pressure-induced crystallization, which requires no humid atmosphere or high temperature. Although pressure-induced crystallization at ambient temperature has been reported for some amorphous alloys,[20,21] elemental substances,[22,23] and a chloride,[24] the present report is the first to describe pressure-induced crystallization from amorphous carbonate at much lower pressures than those previously reported.

Based on the method of Koga et al. (1998), ACC was synthesized.[19] Ten milliliter aqueous solutions of Na_2CO_3 (0.1 M) and $CaCl_2$ (0.1 M) were kept in ice water. These chilled solutions were mixed and shaken rapidly. The precipitates were filtered immediately using a membrane filter (ϕ 0.45 μm) and washed twice with 10 mL of acetone. The precipitates were dried in a desiccator evacuated with a diaphragm pump (ca. 10^2 Pa) for one day. A part of the dried precipitates was kept under higher vacuum conditions using a turbomolecular pump (ca. 10^{-3} Pa) for one day to produce an ACC sample with less H_2O content. All solutions were prepared using Milli-Q water (>18.2 Ω·m). All reagents were obtained from Wako Pure Chemical Industries Ltd.

Water contents in the synthesized ACCs were determined from weight loss shown in TG-DTA measurements (TG-8120; Rigaku Corp.). Approximately 10 mg samples were weighed into an alumina pan (5 mm diameter, 5 mm height). Measurements were performed at temperatures of room temperature to 1000 °C at a heating rate of 10 K min^{-1} under flowing N_2 gas (130 cm^3 min^{-1}). For measurements, alumina powder was used as a reference. The obtained TG-DTA data are shown in the Supporting Information (SI).

The synthesized ACCs were pressurized using a hydraulic press in a tungsten carbide piston-cylinder of 4 mm inner

Received: December 28, 2011
Revised: June 12, 2012
Published: June 18, 2012

diameter. No pressure medium was used in the sample chamber; the compression was uniaxial. The load was maintained for 10 min in each run. Pressure applied to the samples was estimated from the load of the press and the contact area between the piston and the sample. In this study, the pressure conditions were 0.1−800 MPa. All experiments were performed at room temperature.

Powder X-ray diffraction (XRD) patterns of the synthesized ACC and the recovered samples were obtained on a silicon zero background plate using an X-ray diffractometer (Miniflex; Rigaku Corp.). For samples recovered from high pressure, the XRD analyses were performed after keeping the samples in a vacuum desiccator that had been evacuated using the diaphragm pump for one night.

IR adsorption spectra of a synthesized ACC were obtained using two independent procedures: the KBr-pellet method in transmission mode using an FT-IR spectrometer (Spectrum GX, PerkinElmer Inc.) and the attenuated total reflection (ATR) method on an FT-IR spectrometer (Spectrum One, PerkinElmer Inc.).

Figure 1 depicts XRD patterns of synthesized ACCs before compression and the samples recovered after compression at high pressures. These as-grown ACC samples indicate no distinct diffraction peaks in the XRD patterns, but they do show some broad halos that are specific to amorphous materials including ACC (see the bottom spectra in Figure 1).[3] From the weight loss in the TG curves, H_2O contents in the two ACC samples dried using the diaphragm pump were determined as 21 wt % and 17 wt % (see SI Figures S1(a) and S1(b)). The samples were independently prepared in the same way described above. A part of the ACC sample with H_2O content, 21 wt %, was kept in the vacuum chamber evacuated using the turbomolecular pump (ca. 10^{-3} Pa) for one day. The H_2O content decreased to 10 wt % by the additional drying (see Figure S1(c)). Hereinafter, the ACCs are designated respectively as high-H_2O ACC (21 wt %), middle-H_2O ACC (17 wt %), and low-H_2O ACC (10 wt %). Figure 2 depicts differential TG (DTG)-curves of the three types of ACCs. The curves show a main peak at 85 °C and a shoulder peak at the higher temperature up to 250 °C. The main peak weakened with decreased H_2O contents depending on vacuum conditions. In particular, the main peak of low-H_2O ACC critically weakened and almost disappeared. However, the shape and intensity of the shoulder peaks mutually coincided at higher temperatures, irrespective of the H_2O contents. These results imply the existence of two types of H_2O in the ACCs: weakly bound H_2O and tightly bound H_2O.[25] We presume these two types of H_2O respectively as adsorbed H_2O and structural H_2O.

Some XRD patterns of ACCs after compression present sharp peaks corresponding to crystalline phases of calcium carbonate: calcite and vaterite (Figure 1). These results demonstrate that ACC is crystallized by the compression: pressure-induced crystallization. The crystallized pressures of high-, middle-, and low-H_2O ACCs were, respectively, 240 MPa, 400 MPa, and 640 MPa. The crystallized pressure increased continuously with decreased H_2O contents. These results indicate that the H_2O in the ACC, the adsorbed H_2O in particular, promotes the pressure-induced crystallization.

We measured TG-DTA on the middle-H_2O ACC samples after compression at 400 and 800 MPa (see Figure S1). The TG-DTA data showed that the compressed samples completely crystallized and that it contained a considerable amount of H_2O (see Figure S1). The remaining H_2O contents of the samples compressed at 400 and 800 MPa were, respectively, 8 wt % and 3 wt %. Moreover, we observed no considerable weight loss at less than 130 °C in the TG-curve of the sample compressed at 800 MPa (see Figure S1(e)). These results suggest that H_2O exists in the crystalline grains after crystallization.

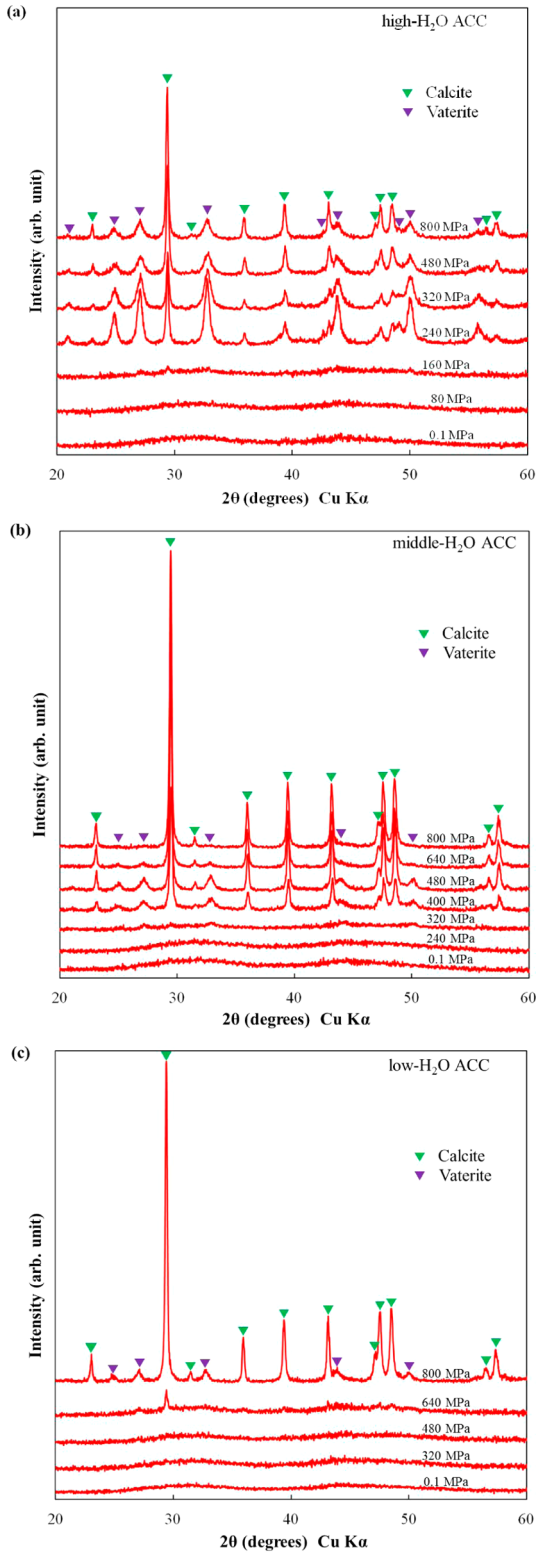

Figure 1. XRD patterns of the synthesized ACCs and compressed samples: (a) high-H_2O ACC; (b) middle-H_2O ACC; (c) low-H_2O ACC.

dx.doi.org/10.1021/cg2017159 | *Cryst. Growth Des.* 2012, 12, 3357−3361

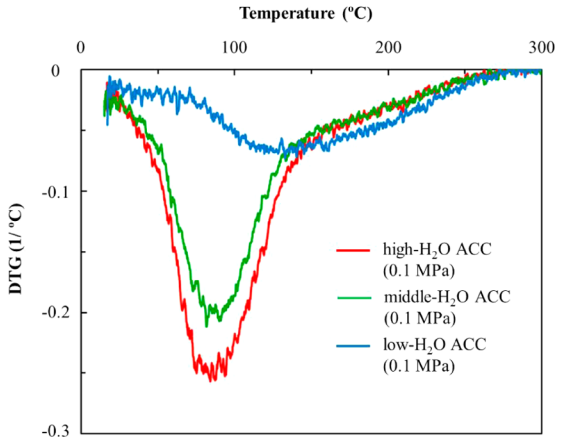

Figure 2. Differential TG (DTG)-curves of the synthesized ACCs. The curves were smoothed using a moving average.

In most crystallized samples, we detected vaterite: a metastable phase of calcium carbonate. In the case of crystallization from a supersaturated aqueous solution, vaterite metastably appears in an early stage of $CaCO_3$ precipitation according to the Ostwald step rule.[1,4,13,26−29] The metastable phase might have kinetic advantages: a lower surface energy and a lower activation barrier.[26] The precipitated vaterite dissolves gradually and precipitates as a more stable phase, e.g. calcite, with time and with the decrease of supersaturation in the solution. By analogy with the crystallization from the supersaturated solution, the appearance of metastable vaterite means that thermodynamically equilibrium condition was not achieved in the samples during compression and that the crystallization was mainly or partially dominated by kinetics. Therefore, we unify the compression duration in all the runs to facilitate mutual comparison.

The relative abundance between calcite and vaterite can be estimated from the intensity ratio of diffraction peaks of these polymorphs in the XRD patterns.[30] The estimated relative abundances are presented in Table 1. The relative abundance of calcite increased concomitantly with increased compression pressure (Table 1). Under ambient pressure, the calcite density (2.710 g/cm^3) is greater than that of vaterite (2.650 g/cm^3).[31,32] Therefore, the preferential appearance of calcite at higher pressure might be reasonable. The density of aragonite is 2.930 g/cm^3 under ambient pressure, which is greatest in the crystalline phases of calcium carbonate.[33] Crystallization of aragonite in pressure-induced crystallization is expected at higher pressure because of the dense structure.

Table 1. Relative Abundance of Calcite and Vaterite in the Crystallized Samples

pressure/MPa	$X_{Calcite}/X_{Vaterite}$ (from high-H_2O ACC)	$X_{Calcite}/X_{Vaterite}$ (from middle-H_2O ACC)	$X_{Calcite}/X_{Vaterite}$ (from low-H_2O ACC)
240	0.27 ± 0.03	*b*	*b*
320	0.33 ± 0.04	*b*	*b*
400	*a*	3.1 ± 0.5	*b*
480	1.4 ± 0.2	5.1 ± 0.7	*b*
640	*a*	*c*	*c*
800	2.2 ± 0.3	*c*	8.4 ± 1.7

[a]There are no data. [b]Crystalline phase was not detected. [c]Vaterite phase was not detected.

Comparison of the relative abundance of calcite after compression among the three types of ACCs indicates that the H_2O contents affect the relative abundance (see Table 1). The calcite abundance of middle-H_2O ACC after the compression at 480 MPa was higher than that of high-H_2O ACC. Similarly, the calcite abundance of low-H_2O ACCs after compression at 800 MPa was substantially higher than that from the high-H_2O. As described above, the difference of H_2O contents was attributable to the amount of adsorbed H_2O. The adsorbed H_2O primarily affects the relative abundance of calcite to vaterite after compression. The possibility exists that the interfacial energy of the crystalline phases might be changed by the adsorbed H_2O. Consequently, vaterite might have a kinetic advantage, as in the case of crystallization from supersaturated solution. The contribution of the adsorbed H_2O to the interfacial energy was described in a previous report of thermal crystallization from ACC.[25] The previous study indicated that preferential adsorption of H_2O on a specific calcite surface promotes the formation of an oriented $CaCO_3$ film in the thermal crystallization. The correlation between the crystallization pressure and the H_2O content can also be associated with the change of interfacial energy caused by the adsorbed H_2O. The lower surface energy is favorable for nucleation of the crystalline phase, at least in the solution condition.[26] The results of this study suggest that the polymorphs are controlled thermodynamically and kinetically, and they imply the possibility of controlling the polymorphs through adjustment of the following factors in pressure-induced crystallization: the H_2O content in ACC, the compression pressure, and the compression duration.

The pressure-induced crystallization provides a technical caution related to measurements of IR absorption spectra of ACC. Infrared spectroscopy has been used in important studies examining biogenic ACC and synthetic ACC.[2,3,5−12,34−37] For obtaining IR absorption spectra, the KBr-pellet method is applied in general. For preparing a KBr pellet, a sample is ground and compressed with KBr, which might induce an artifact: crystallization from ACC during the preparation process. To evaluate the artifact, we compared the IR absorption spectra of high-H_2O ACC obtained from the KBr pellet after compression and from ATR measurement on a raw sample. The KBr pellet was prepared from ACC mixed with KBr by a compression using a hand press. In the preparation, we ground the KBr crystal but did not grind the mixture. KBr powder and ACC were mixed gently with a spatula to avoid the artifacts. Figure 3 portrays IR spectra of synthesized high-H_2O ACC obtained using the two methods. The IR spectrum obtained using the ATR method coincided with that of the typical ACC reported previously.[3] In contrast, the IR spectrum obtained from the KBr technique shows narrow peaks at 713 cm^{-1} and 745 cm^{-1}, which respectively correspond to the crystalline phases: calcite and vaterite.[3,38] In addition, the out-of-plane bending peak at 866 cm^{-1} was shifted to 876 cm^{-1}, which corresponds to the ν_2 mode of calcite (875 cm^{-1}) and vaterite (877 cm^{-1}).[3,38] These results indicate that the compression in the preparation for the KBr pellet can affect the IR data and that the pressure-induced crystallization can occur during the sample preparation. According to a review of the FT-IR, the recommended pressure for formation of KBr pellets is about 420 MPa,[39] which is comparable to the crystallized pressure of high-H_2O ACC and middle-H_2O ACC. The pressure-induced crystallization can be triggered sufficiently by the compression in the preparation of the KBr-pellet.

dx.doi.org/10.1021/cg2017159 | Cryst. Growth Des. 2012, 12, 3357−3361

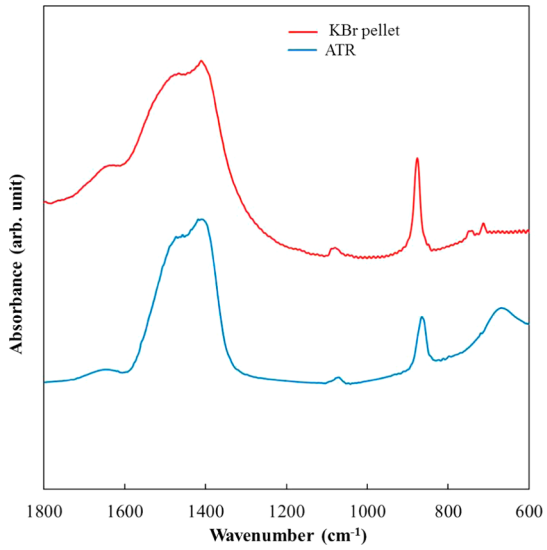

Figure 3. IR spectra of high-H_2O ACC. The spectrum obtained from the ATR method shows a broad peak of the symmetric stretch of carbonate ion at 1080 cm^{-1} (ν_1), a broad peak of the carbonate out-of-plane bending at 866 cm^{-1} (ν_2), and a split peak of the asymmetric stretch of the carbonate ion around 1450 cm^{-1} (ν_3). In addition, the in-plane bending at 713 cm^{-1} (ν_4) is broadened and shifted to a lower wavenumber. These peak positions, peak broadening, and peak shift coincide with the reported IR spectra of ACC.[3]

The present result suggests that measurement of the IR spectra of ACC requires caution to avoid artifacts produced by the sample preparation.

The pressure-induced crystallization from ACC described herein might open a new avenue for developing functional materials. For instance, the pressure-induced crystallization can be performed simultaneously with the molding process, which engenders flexibility in the material shape. Furthermore, dopant materials might be introduced efficiently to calcium carbonate via the amorphous state.[40] These advantages are expected to be meaningful for the development of new materials.

In summary, crystallization from synthesized ACC was induced by compression. The crystallized pressure depended on the H_2O content of ACC. This result indicates that H_2O in the ACC serves an important role in the pressure-induced crystallization from ACC. Further studies are expected to clarify the role of H_2O and the crystallization mechanism.

■ ASSOCIATED CONTENT

Supporting Information

Results of TG-DTA. This material is available free of charge via the Internet at http://pubs.acs.org.

■ AUTHOR INFORMATION

Corresponding Author

*E-mail: yoshino.toru@iri-tokyo.jp. Phone: +81-(0)3-5530-2646. Fax: +81-(0)3-5530-2629.

Notes

The authors declare no competing financial interest.

■ ACKNOWLEDGMENTS

We are grateful to Dr. K. Komatsu and Dr. M. Arakawa for technical support. This study was supported by a Grant-in-Aid for Creative Scientific Research (19GS0205) from the Japan Society for Promotion of Science (JSPS) and Global COE Programs (Chemistry Innovation through Cooperation of Science and Engineering, The University of Tokyo, and Center for Advanced Experimental and Theoretical Deep Earth Mineralogy, Ehime University) from MEXT in Japan. This study was also supported by KIGAM Basic Research Program.

■ REFERENCES

(1) Ogino, T.; Suzuki, T.; Sawada, K. *Geochim. Cosmochim. Acta* **1987**, *51*, 2757.
(2) Brečević, L.; Nielsen, A. E. *J. Cryst. Growth* **1989**, *98*, 504.
(3) Addadi, L.; Raz, S.; Weiner, S. *Adv. Mater.* **2003**, *15*, 959.
(4) Pontoni, D.; Bolze, J.; Dingenouts, N.; Narayanan, T.; Ballauff, B. *J. Phys. Chem. B* **2003**, *107*, 5123.
(5) Aizenberg, J.; Lambert, G.; Addadi, L.; Weiner, S. *Adv. Mater.* **1996**, *8*, 222.
(6) Beniash, E.; Aizenberg, J.; Addadi, L.; Weiner, S. *Proc. R. London B* **1997**, *264*, 461.
(7) Hasse, B.; Ehrenberg, H.; Marxen, J. C.; Becker, W.; Epple, M. *Chem.—Eur. J.* **2000**, *6*, 3679.
(8) Raz, S.; Testeniere, O.; Hecker, A.; Weiner, S.; Luquet, G. *Biol. Bull.* **2002**, *203*, 269.
(9) Weiss, I. M.; Tuross, N.; Addadi, L.; Weiner, S. J. *Exp. Zool.* **2002**, *293*, 478.
(10) Becker, W.; Bismayer, U.; Epple, M.; Fabritius, H.; Hasse, B.; Shi, J.; Ziegler, A. *J. Chem. Soc., Dalton Trans.* **2003**, 551.
(11) Weiner, S.; Levi-Kalisman, Y.; Raz, S.; Addadi, L. *Connect. Tissue Res.* **2003**, *44*, 214.
(12) Politi, Y.; Arad, T.; Klein, E.; Weiner, S.; Addadi, L. *Science* **2004**, *306*, 1161.
(13) Rieger, J.; Frechen, T.; Cox, G.; Heckmann, W.; Schmidt, C.; Thieme, J. *Faraday Discuss.* **2007**, *136*, 265.
(14) Pouget, E. M.; Bomans, P. H. H.; Goos, J. A. C. M.; Frederik, P. M.; de With, G.; Sommerdijk, N. A. J. M. *Scense* **2009**, *323*, 1455.
(15) Gebauer, D.; Völkel, A.; Cölfen, H. *Scense* **2008**, *322*, 1819.
(16) Gower, L. B. *Chem. Rev.* **2008**, *108*, 4551.
(17) Kim, Y.-Y.; Douglas, E. P.; Gower, L. B. *Langmuir* **2007**, *23*, 4862.
(18) Gower, L. B.; Odam, D. J. *J. Cryst. Growth* **2000**, *210*, 719.
(19) Koga, N.; Nakagoe, Y.; Tanaka, H. *Thermochim. Acta* **1998**, *318*, 239.
(20) He, D.; Zhao, Q.; Wang, W. H.; Che, R. Z.; Liu, J.; Luo, X. J.; Wang, W. K. *J. Non-Cryst. Solids* **2002**, *297*, 84.
(21) Xu, M.; Meng, Y.; Cheng, Y. Q.; Sheng, H. W.; Han, X. D.; Ma, E. *J. Appl. Phys.* **2010**, *108*, 083519.
(22) Yang, K.; Cui, Q.; Hou, Y.; Hou, Y.; Liu, B.; Zhou, Q.; Hu, J.; Mao, H.-K.; Zou, G. *J. Phys.: Condens. Matter* **2007**, *19*, 425220.
(23) Pandey, K. K.; Garg, N.; Shanavas, K. V.; Sharma, S. M.; Sikka, S. K. *J. Appl. Phys.* **2011**, *109*, 113511.
(24) Polsky, C. H.; Martinez, L. M.; Leinenweber, K.; VerHelst, M. A.; Angell, C. A.; Wolf, G. H. *Phys. Rev. B* **2000**, *61*, 5934.
(25) Xu, X.; Han, J. T.; Kim, D. H.; Cho, K. *J. Phys. Chem. B* **2006**, *110*, 2764.
(26) Navrotsky, A. *Proc. Natl. Acad. Sci.* **2004**, *101*, 12096.
(27) Kawano, J.; Shimobayashi, N.; Kitamura, M.; Shinoda, K.; Aikawa, N. *J. Cryst. Growth* **2002**, *237–239*, 419.
(28) Spanos, N.; Koutsoukos, P.-G. *J. Cryst. Growth* **1998**, *191*, 783.
(29) Tsuno, H.; Kagi, H.; Akagi, T. *Bull. Chem. Soc. Jpn.* **2001**, *74*, 479.
(30) Kontoyannis, C. G.; Vagenas, C. G. *Analyst* **2000**, *125*, 251.
(31) Graf, D. L. *Am. Mineral.* **1961**, *46*, 1283.
(32) Kamhi, S. R. *Acta Crystallogr.* **1963**, *16*, 770.
(33) de Villiers, J. P. R. *Am. Mineral.* **1971**, *56*, 758.
(34) Raz, S.; Hamilton, P. C.; Wilt, F. H.; Weiner, S.; Addadi, L. *Adv. Funct. Mater.* **2003**, *13*, 480.
(35) Politi, Y.; Levi-Kalisman, Y.; Raz, S.; Wilt, F.; Addadi, L.; Weiner, S.; Weiner, S.; Sagi, I. *Adv. Funct. Mater.* **2006**, *16*, 1289.

(36) Gebauer, D.; Gunawidjaja, P. N.; Ko, J. Y. P.; Bacsik, Z.; Aziz, B.; Liu, L.; Hu, Y.; Bergström, L.; Tai, C.-W.; Sham, T.-K.; Edén, M.; Hedin, N. *Angew. Chem.* **2010**, *122*, 9037.
(37) Redha, A. V.; Forbes, T. Z.; Killian, C. E.; Gilbert, P. U. P. A.; Navrotsky, A. *Proc. Natl. Acad. Sci. USA* **2010**, *107*, 16438.
(38) Dupont, L.; Portemer, F.; Figlarz, M. *J. Mater. Chem.* **1997**, *7*, 797.
(39) Katon, J. E. *Micron* **1996**, *27*, 303.
(40) Raz, S.; Weiner, S.; Addadi, L. *Adv. Mater.* **2000**, *12*, 38.